Research Article

Journal of PeptideScience

Received: 28 October 2011 Revised: 26 April 2012 Accepted: 26 April 2012 Published online in Wiley Online Library: 28 May 2012

(wileyonlinelibrary.com) DOI 10.1002/psc.2420

Designed synthetic analogs of the α-helical peptide temporin-La with improved antitumor efficacies via charge modification and incorporation of the integrin αvβ3 homing domain

Yuwen Diao, Wenyu Han,* Honglei Zhao, Seng Zhu, Xiaohe Liu, Xin Feng, Jingmin Gu, Cuimei Yao, Shanshan Liu, Changjiang Sun and Fengguang Pan

How to target cancer cells with high specificity and kill cancer cells with high efficiency remains an urgent demand for anticancer drugs. Temporin-La, which belongs to the family of temporins, presents antitumor activity against many cancer cell lines. We first used a whole bioinformatic analysis method as a platform to identify new anticancer antimicrobial peptides (AMPs). On the basis of these results, we designed a temporin-La analog (temporin-Las) and related constructs containing the Arg-Gly-Asp (RGD) tripeptide, the integrin αvβ3 homing domain (RGD-La and RGD-Las). We detected a link between the net charges and integrin αvβ3 expression of cancer cell lines and the antitumor activities of these peptides. Temporin-La and its synthetic analogs inhibited cancer cell proliferation in a dose-dependent manner. Evidence was provided that the affinity between RGD-Las and tumor cell membranes was stronger than other tested peptides using a pull-down assay. Morphological changes on the cell membrane induced by temporin-La and RDG-Las, respectively, were examined by scanning electron microscopy. Additionally, time-dependent morphological changes were detected by confocal microscopy, where the binding process of RGD-Las to the cell membrane could be monitored. The results indicate that the electrostatic interaction between these cationic peptides and the anionic cell membrane is a major determinant of selective cell killing. Thus, the RGD tripeptide is a valuable ligand motif for tumor targeting, which leads to an increased anticancer efficiency by RGD-Las. These AMP-derived peptides have clinical potential as specifically targeting agents for the treatment of αvβ3 positive tumors.

Supporting information can be found in the online version of this article.

Keywords: antimicrobial peptides; bioinformatic analysis; integrin αvβ3; net charge; antitumor activities

Introduction

Cancer remains a leading cause of early mortality worldwide, accounting for 7.4 million deaths (around 13% of all deaths) every year (http://www.who.int/). Although many chemotherapeutic agents have been developed, most have deleterious side effects [1–4] because they are cytotoxic to both cancer cells and healthy cells and tissues [5]. A large and growing number of studies have shown that some bioactive peptides can kill cancer cells directly with low cytotoxicity to normal cells. Antimicrobial peptides (AMPs) derived from various species (including insects, amphibians, and especially humans) are bioactive peptides [6] with potential applications as anticancer agents. Hoskin and Ramamoorthy categorized anticancer AMPs by secondary structure and suggested that α-helical anticancer peptides are of great potential [7]. Cecropin A and B, aurein 1.2, citropin 1.1, gaegurins, magainins, and magainin analogs have been reported to be selectively cytotoxic against human cancer cells [7–10].

The AMPs isolated from nature and their synthetic mimics are specifically active against many pathogens, such as bacteria, viruses, fungi, and protozoa [6,11–14]. To date, more than 500 antimicrobial peptides have been identified, but most studies have focused on the antimicrobial activity and selectivity of the AMPs [15–18]. These antimicrobial properties also present new opportunities for use as anticancer agents. As new candidates for anticancer drugs, AMPs possess the advantages of high positive charges, amphipathic α-helices, short amino acid sequences, low molecular weights, and weak antigenicity [19]. These unique properties of some AMPs may allow these agents to be cytotoxic against tumor cells but nonhemolytic and weakly cytotoxic against nontumor cells. There is thus considerable interest in developing AMPs or analogs with anticancer activity as therapeutic agents [20,21]. Many structure–activity studies on small linear antibacterial peptides indicated that the net positive

* *Correspondence to: Wenyu Han, College of Animal Science and Veterinary Medicine, Jilin University, Xi'an Road 5333#, Changchun 130062, China. E-mail: hanwy@jlu.edu.cn*

College of Animal Science and Veterinary Medicine, Jilin University, Changchun 130062, China

Journal of PeptideScience

charges, hydrophobicity, amphiphilicity, and α-helical structure were the most important factors conferring activity and specificity against pathogens. Dennison *et al*. recently used a variety of bioinformatic techniques to identify properties that may contribute to differences in efficacy and selectivity of those AMPs with anticancer activities [21]. The cell membranes of malignant tumor cells and normal cells can be quite distinct. Malignant tumor cell membranes typically carry net negative charges due to a higher than normal expression of anionic molecules such as phosphatidylserine [22] and O-glycosylated mucins [23]. The net negative charges may be one of the most obvious differences that could be exploited for specific cell targeting [24] as the ability of certain AMPs to kill cancer cells selectively was related to the anionic malignant tumor cell membranes [19]. Indeed, the electrostatic interactions between cationic AMPs and anionic cell membrane components are believed to be a major factor in the selective killing of cancer cells by the AMPs [18,20]. A range of physiochemical characteristics, however, are involved in determining the efficacy and selectivity of the anticancer AMPs. Herein, we used a whole bioinformatic analysis method as a platform for identifying new anticancer AMPs. We also used factor analysis to investigate the independence of each physicochemical characteristic and to determine if changing only one physicochemical parameter (e.g., net charges) could regulate the anticancer activity.

In our previous study, we isolated a small antimicrobial peptide belonging to the temporins, temporin-La, which showed strong antimicrobial activities against many bacteria tested, especially Gram-positive bacteria, and presented strong antitumor activity [25]. In addition, temporin-La showed no hemolytic activity against rabbit erythrocytes at 250 mg/l. All temporins previously reported are small (between 10 and 18 amino acids), hydrophobic, and C-terminally amidated. Temporin-La is a 13-membered peptide with a molecular weight of 1623.08 Da. Temporin-La has a net charge of +3 at pH 7.0, whereas most other temporins have net charges <+2. Like other temporins, the C-terminus of temporin-La is amidated [25].

In this study, we first analyzed anticancer AMPs by bioinformatics. Factor analysis was used to determine how six parameters (net positive charges, percent hydrophobic residues, mean hydrophobicity <H>, grand average of hydropathicity, amphiphilicity <μH>, and secondary structure) contributed to structure and activity relationship. We then predicted and calculated the five parameters and the 3D mimic images of designed peptides by bioinformatic analysis. Our second aim was to evaluate the potency of electrostatic interactions with the high net negative surface charges of tumor cells. For this purpose, the antitumor activity of designed peptides on different human cancer cell lines was measured by 3-(4,5-dimethylthiazol-2-yl)-2,5-diphenyltetrazolium bromide assay (MTT) assays to examine the effects on cell proliferation. Furthermore, the cell potentials of cell lines and control cells were determined in order to compare net negative charges. The morphological changes of the cell membrane induced by temporin-La and temporin-La analogs was determined by scanning electron microscopy (SEM). The time-dependent morphological changes were detected by confocal microscopy, where the binding of temporin-La analogs to the cell membrane was monitored. The results revealed increased anticancer efficiency of these analogs suggesting clinical potential as specifically targeted anticancer agents.

Materials and Methods

Bioinformatic Analysis of Antitumor AMPs

Database and parameters

Ninety-two AMPs with antitumor activities were retrieved from the antimicrobial peptide database originally created by Zhe Wang in his Master thesis under the direction of Dr. Gus Wang [26] (see Table S1). The characteristics assessed were net positive charges, percent hydrophobic residues, hydrophobicity [(both the corresponding mean hydrophobicity <H> and the grand average of hydropathicity (GRAVY)], amphiphilicity (the mean hydrophobic moment, <μH>), and secondary structure [27–31]. The HeliQuest web server (http://heliquest.ipmc.cnrs.fr/) and ExPASy Proteomics Server (http://www.expasy.ch/cgi-bin/protparam) were used to calculate structural and physicochemical parameters [32].

Statistical analysis of antitumor AMPs

Histograms were used for showing the distribution of the six parameters. Factor analysis was used to determine how the five parameters contributed to structure–activity relationship. The SPSS statistical software package version 13.0 (SPSS, Inc., Chicago, IL) was used for all statistical analyses. The temporins (47) were obtained from the Expasy protein database, and some were summarized by M. L. Mangoni [37]. In addition, five new temporins named temporin-La, temporin-Lb, temporin-1Ca2, temporin-1Cb2, and temporin-1Cc2 were identified and cloned from *Lithobates catesbeianus* by our lab (Table 1). Sequence characteristics and relationships among the resulting 52 temporin peptides were revealed by alignment using MEGA software (see Table S3) [33].

Design of the Analog Peptides

The protein sequence analysis software ANTHEPROT was used for predicting the secondary structure of the designed peptides [34]. Helical wheel project was used to reveal the distribution of

Table 1. Primary structure, net charge, molecular masses, and isoelectric points of five temporin peptides isolated in our laboratory

Peptides	Sequence	Net positive charge (PH = 7.4)	MW	Theoretical p*I*
Temporin-La	LLRHVVKILEKYL	3	1624.0	9.7
Temporin-Las	LLRHVVKILSKYL	4	1582.0	10.29
Temporin-1Ca2	FLTFPGMTFGKLL	1	1471.8	8.75
Temporin-1Cb2	FLFPLITSFLSKFL	1	1673.0	8.75
Temporin-1Cc2	FLFPLLASFLGKVL	1	1564.9	8.75

cationic amino acids on the hydrophilic surface [34]. The 3D structure of the designed peptides was predicted by CHEM BIOOFFICE 8.0 (CambridgeSoft Corporation, USA) [35].

Peptide Synthesis

All peptides were synthesized by GL Biochem (Shanghai) Ltd. using standard Fmoc chemistry and purified by HPLC to >90% homogeneity (Table 2). Temporin-La and RGD-Las were fluorescein isothiocyanate (FITC)-labeled at the N-terminus. Peptide stock solutions were prepared in phosphate-buffered saline (PBS, pH 7.4).

Cell Lines and Culture

Human lung adenocarcinoma epithelial cell line (A549), human colorectal carcinoma cell line (SW1116), human gastric carcinoma cell line (BGC-823), human epithelial carcinoma cell line (Hela), human hepatocellular liver carcinoma cell line (HepG2), human hepatocarcinoma cell line (SMMC-7721), human embryonic kidney cell line (HEK 293T), human liver cell line (HL-7702), bovine mammary epithelial cells (MECs), and peripheral blood mononuclear cell (PBMC) were all kept in RPMI1640 media (pH 7.2) supplemented with 10% fetal bovine serum at 37 °C in a humidified atmosphere of 5% CO_2 in air and in absence of antibiotics. All human cancer cell lines were obtained by courtesy of Dr. Yu (Changchun University of Science and Technology).

Cytotoxicity Assay

Growth inhibition in the presence of individual temporin peptides or constructs was evaluated using the MTT assay. All the cell lines were seeded onto 96-well plates at a density of 5.0×10^3 cells in a final volume of 100 μl medium. Various concentrations of tested peptides (3.125, 6.25, 12.5, 25, 50, 100 μg/ml) were prepared from the stock solution and added 12 h later, and the plates were incubated for 36 h at 37 °C. Subsequently, 20 μl of MTT at a concentration of 5 mg/ml in PBS (pH 7.4) was added to each well, and the cells were incubated for an additional 4 h at 37 °C. The supernatants were aspirated, and 150 μl of DMSO was added to each of the wells to dissolve the formazan crystals created by viable cells from MTT under shaking for 10 min to dissolve any remaining precipitate. The UV absorbance was determined using an ELX800 reader (Bio-Tek instruments, Inc., Winooski, VT) at 490 nm. The mean absorbance of control wells represented 100% cell survival, and the mean absorbance of treated cells was calculated relative to control values to determine tumor line sensitivity to each peptide. Each MTT detection assay was repeated in triplicate, and the relative activity was calculated by relative activity (%) = [1 − (test-background)/(control-background)] × 100%.

Hemolytic Activity Assay

Hemolytic activity of each peptide was tested using rabbit erythrocytes and human red blood cells (hRBCs) from healthy donors in media according to the method previously reported [36]. Briefly, serially diluted peptides were incubated with washed rabbit erythrocytes and hRBCs at 37 °C for 30 min. The cells were then centrifuged, and the 595 nm absorbance of the supernatant was measured. Maximum hemolysis was determined in rabbit erythrocytes and hRBCs treated with 1% Triton X-100. The controls for zero hemolysis (blank) were obtained from hRBCs suspended in PBS. Each measurement was conducted in triplicate.

Table 2. Analytical data of the synthetic temporin peptides

Peptides	HPLC, R_t (s)	Column	Gradient			MW	Method
La	13.525	4.6*250 mn, Venusil XBP-C18		A	B	1623.08	ESI
			0.1 min	23%	77%		
			25 min	48%	52%		
			25.01 min	100%	0%		
			30 min	Stop	Stop		
Las	13.647	4.6*250 mn, VYDAC-C18		A	B	1581.04	ESI
			0.1 min	10%	90%		
			25 min	35%	65%		
			25.01 min	100%	0%		
			30 min	Stop	Stop		
RGD-La	13.273	4.6*250 mn, VYDAC-C18		A	B	1951.41	ESI
			0.1 min	30%	70%		
			25 min	55%	45%		
			25.01 min	100%	0%		
			30 min	Stop	Stop		
RGD-Las	11.678	4.6*250 mn, VYDAC-C18		A	B	1909.37	ESI
			0.1 min	30%	70%		
			25 min	55%	45%		
			25.01 min	100%	0%		
			30 min	Stop	Stop		

The HPLC condition: solvent A, 0.1% TFA in 100% acetonitrile; solvent B, 0.1% TFA in water; flow rate, 1.0 ml/min; wavelength, 220 nm; volume, La (5 μl), others (20 μl).

Journal of PeptideScience

Zeta Potential Measurement of the Cell Lines

All the cell lines were seeded onto six-well plates at a density of 5.0×10^6 cells in a final volume of 3 ml of medium. When cells were at about 90% confluence, they were collected, centrifuged, and resuspended in 5% dextrose. Net cell surface charges (the cell zeta potential) was measured by Nano ZS (Malvern, UK).

Peptide-cell Pull-down Experiments

All the cell lines were seeded onto 96-well plates at a density of 5.0×10^3 cells/well in a final volume of 100 μl medium. The FITC-labeled peptides (25, 50, 100 μg/ml) were added 12 h later, and the plates were further incubated for 15 to 30 min at 37 °C. The supernatant was carefully removed and pipetted into black microplates. The fluorescence intensities were measured by a fluorescence microplate reader (Spectra Fluor plus, Tecan Austria GmbH, Austria) using an excitation wavelength of 480 nm and emission wavelength of 520 nm.

Time-dependent Membrane Binding and Permeating of the Peptides

The individual peptides (FITC-temporin-La and FITC-temporin-Las) were added to cell monolayers at concentrations of 25 μg/ml. Cells were counterstained for 10 min with 1% Hoechst 33258 stain. Peptide binding was detected every 10 min over 3 h under the confocal microscope (Olympus FluoView FV1000, Olympus, Japan). Images were analyzed using Olympus FLUOVIEW Ver.116 Viewer software.

Morphological Changes of the Cells

Sterilized cover slips were placed in the bottom of 12-well plates. At least 4.0×10^4 cells/ml of SMMC-7721 cells were seeded in

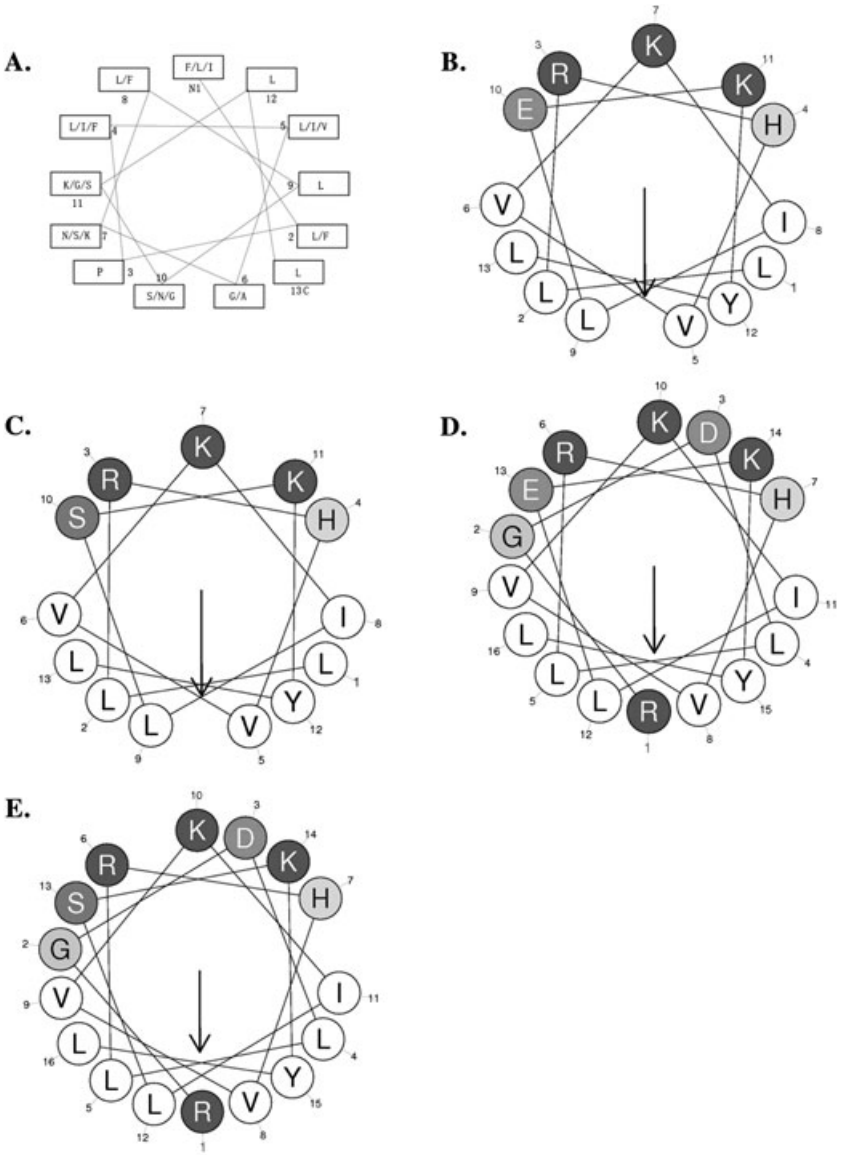

Figure 1. Prediction of amphiphilicity of the designed peptides, and distribution of hydrophobic and hydrophilic amino acid residues on the helix wheel: (A) template of the family of temporins; (B) temporin-La; (C) temporin-Las; (D) RGD-La; (E) RGD-Las.

each well and covered with 3 ml RPMI1640 medium. The plates were then incubated for 36 h at 37 °C. Temporin-La or temporin-Las (at a final concentration of 25 μg/ml) were added on the following day, and plates were incubated for 0.5 h. The medium containing temporin-La and temporin-Las was then removed, and 1 ml of 2.5% glutaraldehyde solution was added to each well to fix the samples. The samples were then sent to Changchun Institute of Applied Chemistry to be analyzed by SEM (XL30ESEM-FEG, FEI, Holland).

Results

Design, Synthesis, and Characterization of the Peptides

On the basis of results of the bioinformatic analysis, the frequency of each type of residue was determined at each position of the temporins listed in Table S3. For this purpose, the peptides were grouped as follows: F/L/I + L/F + P + L/I/F + L/I/V + G/A + N/S/K + L/F + L + S/N/G + K/G/S + L + L. From this grouping, the helix wheel of the template (Figure 1A) was derived. The hydrophobic residues were at positions 1, 2, 4, 5, 8, 9, 12, and 13. Polar residues with positive charges were most common at position 3, 7, and 11, and position 10 was the most common site for polar residues with no charges or negative charges. Correspondingly, Glu-10 was replaced by a Ser residue (temporin-Las), and this analog and the parent temporin-La were extended N-terminally with RGD without spacing to incorporate into the temporin sequence the integrin αvβ3 homing domain (RGD-La and Regd-Las).

The sequences of temporin-La and analogs are reported in Table 3 with their structural parameters. The related helical wheels shown in Figure 1B–E show the distribution of charged and uncharged residues. All the peptides fitted the analysis. The 3D structures of the four peptides were predicted by ChemBioOffice 2008 (CambridgeSoft, Cambridge, MA). The 3D structures were energy minimized in an MM2 force field. All the predictions were carried under in aqueous environment (Figure 2). We found that the RGD tripeptide portion formed a turn-like structure at the N-terminus (Figure 2E), and all temporin peptides adopted an α-helical secondary structure. It is important to note that the positively charged residues Arg-6, Lys-10, and Lys-14 were at one side of each peptide in the 3D structures. These results were in agreement with the prediction of antheprot software and the helical wheel description.

Table 3. Sequences and structural parameters of the synthetic temporin peptides

Peptides	Sequence	Net positive charge	Hydrophobic residue (%)	<H>/<μH>	GRAVY	α-helicity* (%)
Temporin-La	LLRHVVKILEKYL	3	61.54	0.654/0.754	0.600	100
Temporin-Las	LLRHVVKILSKYL	4	61.54	0.700/0.730	0.808	100
RGD-temporin-La	RGDLLRHVVKILEKYL	3	50	0.420/0.594	−0.293	94
RGD-temporin-Las	RGDLLRHVVKILSKYL	4	50	0.457/0.575	0.131	94
RGD	RGD	–	–	–	–	–

All peptides were synthesized with an amidated C-terminus except the RGD peptides.
* The α-helicity was calculated by antheprot software using the method of GIB (The secondary structure prediction method) [44].

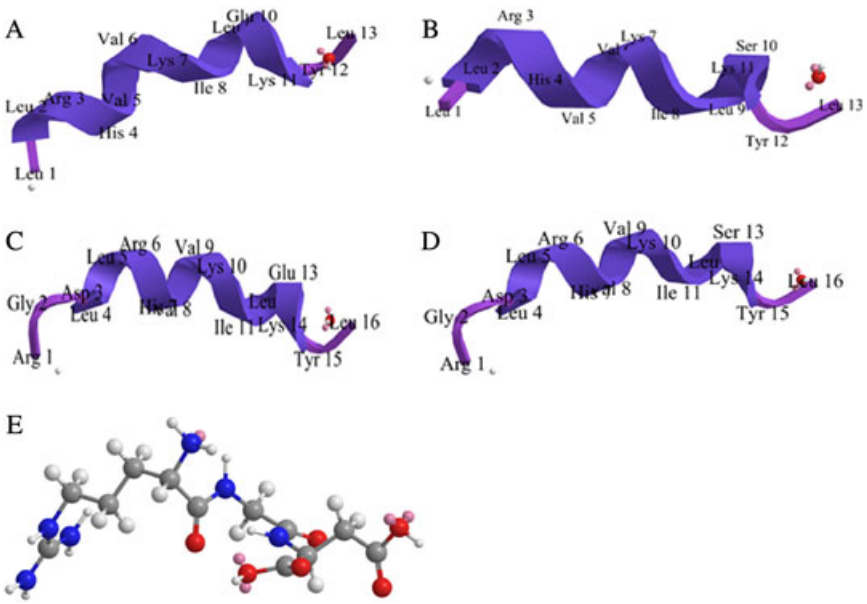

Figure 2. Prediction of the 3D structures of the designed peptides and distribution of hydrophobic and hydrophilic amino acid residues on the secondary structure. Charged amino acids are also marked: (A) temporin-La; (B) temporin-Las; (C) RGD-La; (D) RGD-Las; (E) RGD.

Journal of PeptideScience

Cell Proliferation and Cytotoxicity against Tumor and Normal Cells

All four bioactive peptides inhibited cell proliferation in a dose-dependent manner (Figure 3). There were significant differences in the sensitivity of the tested cancer cell lines to each peptide. The SW1116 cancer cell line was the most sensitive to temporin-La and temporin-Las (Figure 3M,N), and temporin-Las showed higher inhibition than temporin-La (Figure 3J). The A549 cancer cell line had the least sensitivity to temporin-La and temporin-Las (Figure 3M,N). Antitumor activity of RGD-Las was stronger than RGD-La for all the cancer cell lines. The RGD-Las had the highest inhibitory activity against SMMC-7721 and the second highest against SW1116 (Figure 3L). All peptides showed little effects on the proliferation of the 293T human embryonic kidney cell line, MECs, and human lymphomonocytes at concentrations of less than 50 μg/ml (Table 4). All the peptides we tested showed no hemolytic activity against rabbit erythrocytes and human erythrocytes at 250 μg/ml.

Measurement of the Net Charges of Cell Lines

Measurement of zeta potential is used to assess the charge stability of a disperse system, so zeta potential may be related

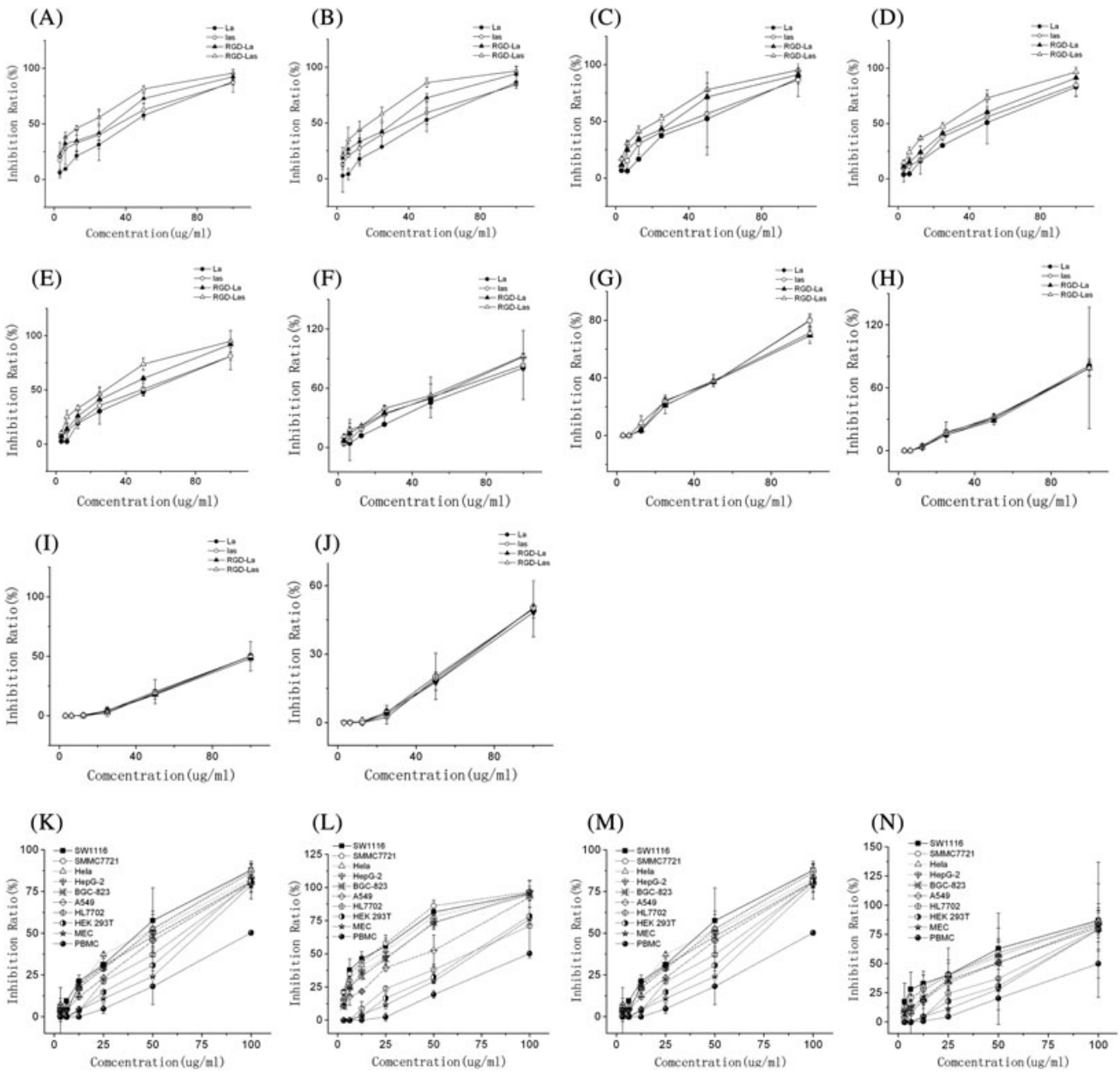

Figure 3. Cell inhibition ratio curves as measured by MTT assays for the four peptides tested against the ten different cells SW1116 (A), SMMC7721 (B), Hela (C), HepG-2 (D), BGC-823 (E), A549 (F), HL7702 (G), HEK-293T (H), MEC (I), and PBMC (J). Comparison of the sensitivity of the 10 cell lines to the peptides RGD-La (K), RGD-Las (L), temporin-La (M), and temporin-Las (N). Cells were incubated in the presence of various concentrations of tested peptides (3.125–100 μg/ml) for 24 h at 37 °C. As a control, cells were cultured without peptide. The mean absorbance of the control cells represented 100% cell inhibition, and the mean absorbance of treated cells was related to control values to determine sensitivity. Error bars represent standard deviation from mean cell inhibition.

Table 4. The inhibition ratio of the four peptides (50 μg/ml) to different cells

Peptides (50 μg/ml)	SW 1116	SMMC-7721	Hela	HepG-2	BGC-823	A549	HL 7702	HEK-293T	MEC	PBMC
Temporin-La	57.62 ± 3.54	52.77 ± 10.50	52.32 ± 24.93	50.90 ± 1.10	48.19 ± 3.78	45.62 ± 5.90	37.22 ± 0.85	30.82 ± 0.95	24.15 ± 16.97	18.17 ± 1.04
Temporin-Las	62.73 ± 5.66	59.37 ± 10.57	56.81 ± 36.34	55.98 ± 24.38	50.85 ± 5.77	50.64 ± 20.54	37.00 ± 0.85	30.90 ± 4.49	27.99 ± 30.32	20.26 ± 10.15
RGD-La	72.69 ± 4.60	70.39 ± 4.00	73.09 ± 2.04	60.22 ± 4.58	62.49 ± 1.84	47.26 ± 2.75	36.25 ± 5.39	27.86 ± 4.26	19.76 ± 8.65	16.22 ± 3.64
RGD-Las	81.465 ± 2.99	86.175 ± 4.15	78.045 ± 5.48	73.07 ± 3.23	73.705 ± 5.53	52.50 ± 11.62	38.13 ± 4.19	32.52 ± 2.28	29.33 ± 1.39	19.34 ± 2.83

Table 5. Characteristics of the ten cell types

Cells	Zeta potential (mV)	αvβ3 expression
SW1116	−27.3667	++
SMMC7721	−23.95	+++
Hela	−21.9667	++
HepG-2	−20.35	++
BGC-823	−25.5	+
A549	−21.6	+
HL7702	−16.85	−
HEK 293T	−13.1	−
MEC	−10.5	−
PBMC	−9.9	−

to the surface charge in a simple cell system (Table 5). The results were correlated to antitumor peptide sensitivity as revealed by the MTT assay. Temporin-La targeted tumor cells by electrostatic interactions. If the absolute value of the zeta potential was high, then the cytotoxicity of temporin-La was strong. Temporin-Las exhibited stronger antitumor activity than temporin-La, but the trends were similar.

Detection of αvβ3 Expressed on Different Cancer Cell Lines

In order to compare the amount of integrin αvβ3 expressed on the cell surfaces of the different cancer cell lines, cultures were stained with Alexa Fluor® 647 anti-human CD51/61 (αvβ3) antibody (Table 5). All the tumor cell lines expressed higher αvβ3 on the cell surface compared with normal cell lines. The SMMC-7721 cells, Hela cells, and SW1116 cells expressed the highest αvβ3, whereas no αvβ3 expression was detected on the HEK 293 cells, HL-7702, MECs, and PBMCs.

Peptide-cell Pull-down Experiments

Peptide-cell binding data are presented as the percent of the initial FITC-peptide remaining in the supernatant (unbound FITC-peptides) (Figure 4). We found that all the cell lines, which carried net negative charges, bound more than 50% of the

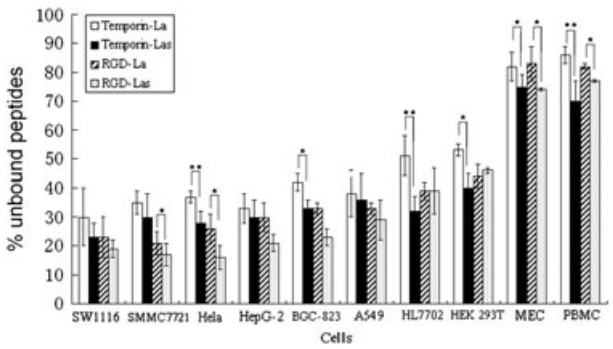

Figure 4. Percentage of initial unbound peptides remaining in the supernatant for the different cells. (□) temporin-La, (■) temporin-Las, (▨) RGD-La, (▩) RGD-Las. ★★$P < 0.01$, ★$P < 0.05$. Independent-sample *T*-test was used. A *P*-value of less than 0.05 was accepted as statistically significant. A *P*-value of less than 0.05 was accepted as statistically extremely significant.

peptide, whereas more than 74% of FITC-peptides remained in the supernatant for MEC and PBMC. Thus, the RGD peptides can bind to tumor cells with higher affinity than to other healthy cells.

The Process of Temporin-La and RGD-Las Binding and Permeabilization of Cell Membranes

Temporin-La and RGD-Las bind to the membrane with nearly the same time course, and there was no clear difference in penetration process as shown by light microscopy (Figure 5A,B). The fringes of SMMC-7721 cells exhibited high fluorescence intensity signals about 40 min after peptide addition. Soon after, the cells were quickly filled with strong fluorescence intensity. In the time course, many intensely fluorescent cell fragments exfoliated. Cells treated with the peptides showed shrinkage, chromatin condensation, and blebbing.

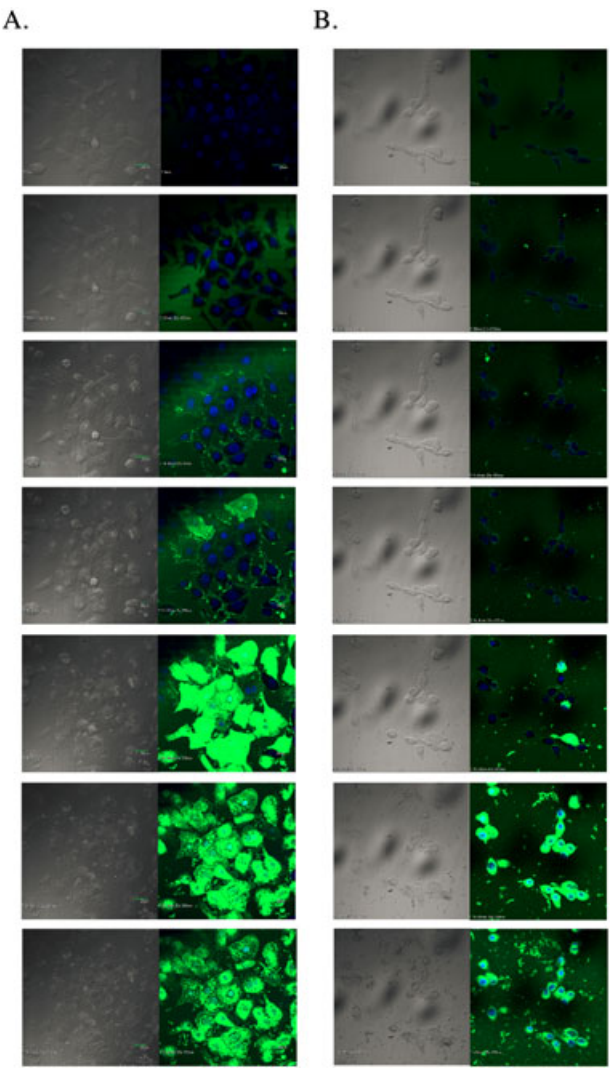

Figure 5. The process of temporin-La and RGD-Las binding and permeabilizing of cell membranes. Confocal microscopy images of time-dependent morphological changes. FITC-labeled peptides (green channel) and SMMC-7721 (blue channel). Light microscopy images of time-dependent morphological change in SMMC-7721. FITC was added as the control; (A) FITC-RGD-Las; (B) FITC-temporin-La.

Morphological Analysis by SEM

Temporin-La and RGD-Las had both common and unique effects on SMMC 7721 cells (Figure 6). Pores were seen in the membranes of treated cells using SEM, whereas untreated cells retained smooth surfaces. The untreated cells were spherical or clostridial in shape and had microvilli on the surface (Figure 6E,F). In contrast, peptide incubation led to dramatic alterations in cellular architecture. The SMMC7721 cells treated with 25 μg/ml bioactive peptide showed disrupted cell membranes, with pore formation and loss of microvilli (Figure 6A–D)

Discussion

Most studies have proven that sequence modifications usually result in complex changes of more than one structural parameter, making it difficult to trace activity differences back to a specific structural motif. The activity of AMPs is thought to be determined by global structural parameters rather than by the specific amino acid sequence [18], but replacement of an amino acid not only changes the sequence but also increases or reduces hydrophobicity, modifies $<\mu H>$, and alters the overall net charge. Our analyses indicated that the histogram of each parameter displays the distribution of a quantitative variable associated with anticancer efficacy.

Factor analysis reveals the structural basis for the design of antimicrobial peptides with enhanced anticancer efficiency. We found that factor 1 (Supporting Information) explains the parameters of percent hydrophobic residues, $<H>$, and GRAVY. These three parameters all concern hydrophobicity, and they contributed 59.2% of the total variance, indicating that hydrophobicity was the most important parameter determining the anticancer efficacy of AMPs, likely because hydrophobicity reflected the affinity to the cell membrane. At the same time, the hydrophobic amino acids formed the hydrophobic helix face, and this structure should enhance membrane disruption. Factor 3 (Supporting Information) explains the parameters of amphiphilicity and $<\mu H>$, and factor 2 the parameters of net charges. These analyses indicated that net charge was relatively more independent than the other four parameters.

Temporins are an important family of antimicrobial peptides first isolated and characterized from *Rana erythraea*. Temporins are the shortest natural antibacterial peptides found to date. It seems that the minimal requirements for antibacterial activity are 13 residues and a net positive charge [37,38]. Alignment of temporins showed conserved sequence properties, and we derived a conserved sequence template (F/L/I + L/F + P + L/I/F + L/I/V + G/A + N/S/K + L/F + L + S/N/G + K/G/S + L + L). We also performed helical wheel plot analysis for the template. We noticed that all the hydrophobic amino acids were concentrated on one side of the helix, whereas polar or hydrophilic amino acids were on the other.

Helix wheel analysis showed that the parent peptide temporin-La had an α-helical structure and high amphiphilicity. Polar residues were all on one side of the wheel, and we found that Glu^{10} was on the same side as the other positive amino acids. We replaced Glu^{10} for Ser^{10} in the hydrophilic helix face of the temporin-La to form the new peptide temporin-Las, which then contained a polar but uncharged residue. The related structural parameters are listed in Table 3. The total net charge increased from +3 to +4, and all the structural parameters were changed

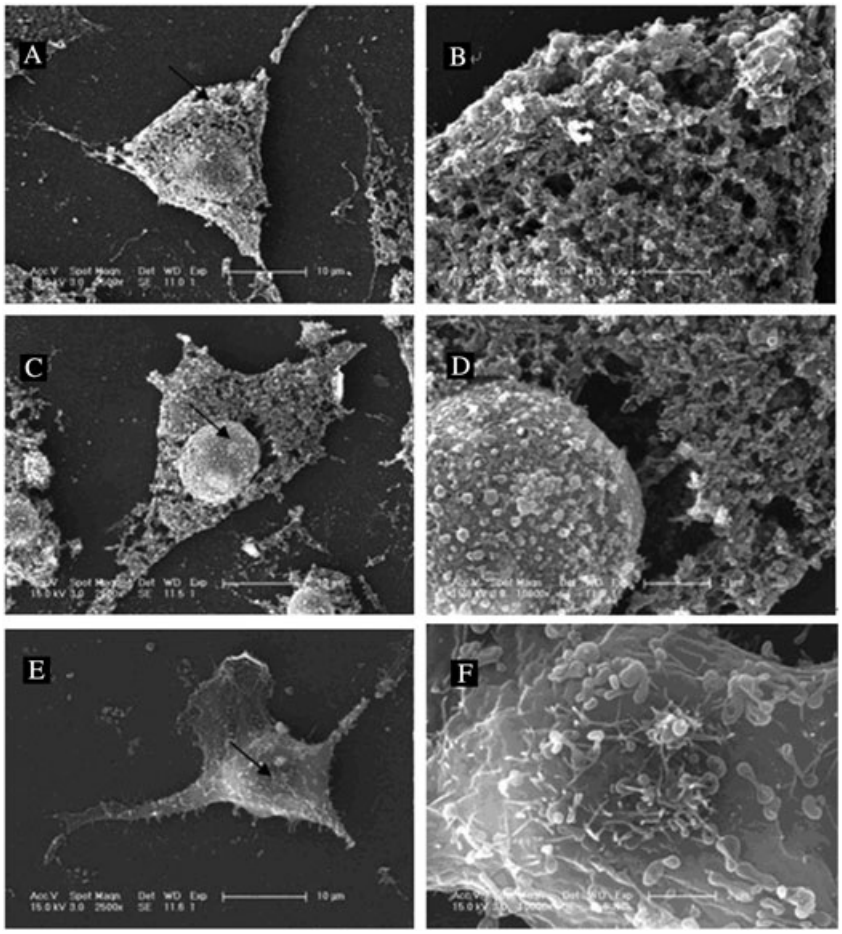

Figure 6. Effect of temporin-La and RGD-Las on the cell membrane in SMMC-7721 cells using scanning electron microscopy. Left panel: SMMC-7721 cells treated with 25 μg/ml temporin-La exhibited disrupted cell membranes (A); SMMC-7721 cells treated with 25 μg/ml RGD-Las exhibited unequally disrupted cell membranes (C); Control SMMC-7721 cells had smooth surfaces and microvilli (E). Right panel: Amplification of each arrow region was at a scale bar of 2 μm (B,D,F).

except percent hydrophobic residues. The hydrophobicity was increased, whereas the amphipathicity was slightly decreased. Although <H> and <μH> of the new peptides were not affected markedly (Table 3), the altered net charge was found to affect the affinity of the peptide to the membrane.

Intrinsic membrane differences also contribute to the sensitivity to specific bioactive peptides [16,20,22,39]. Peptide-cell pull-down experiments revealed that the binding efficiency of temporin-Las (+4) was higher than that of temporin-La (+3), whereas RGD-Las had the strongest affinity (Figure 4). After 30 min, the differences in fluorescence intensities of supernatants and cells surfaces were well evident.

Furthermore, the effect of cell surface charges on peptide affinity was examined. The zeta potential of the cancer cell lines showed that all the cell lines carried negative charges. The SW1116 and SMMC-7721 lines had high zeta potentials, whereas HEK 293T and HL-7702 had low zeta potentials. The zeta potential of primary bovine mammary epithelial cells was nearly neutral. The cytotoxic efficacy of RGD-Las was correlated with the zeta potential (Table 5). These results revealed that the electrostatic peptide-membrane interactions were influenced not only by the positive charges of peptides but also by the negative charges of the cell membranes. Indeed many forces are involved in the interaction of bioactive peptides with cell membranes, such as electrostatic attraction forces, hydrophobic interactions, and van der Waals interactions [40]. The electrostatic attraction between the negatively charged cancer cells and the positively charged bioactive peptides is believed to play a major role in the selective binding and disruption of cancer cell membranes.

Recently, several studies reported the development of radiolabeled RGD peptides for αvβ3 integrin receptor targeting [41–43]. We choose the RGD tripeptide as the targeting motif and the temporin-La and temporin-Las as the cell lysis domain. The total sequence was only 16 amino acids long as we did not use any short peptidic spacer to link the two domains. The RGD itself showed no anticancer activity even at 400 μM (data not shown), but the new chimeric peptides exhibited strong anticancer activity and selectivity to the tumor cells, supporting the working assumption that the RGD tripeptide exerted only tumor targeting functions at the N-terminus of the new chimeric peptides. This assumption was confirmed by measuring αvβ3 expression on the cancer cell lines used in this study. The different fluorescence intensities of each cancer cell indicated different αvβ3 expression levels and that αvβ3 expression (Table 5) correlated well with the efficacy of RGD-Las. The SMMC-7721 cells expressed more αvβ3 on the cell surface than other cells and were also the most sensitive to RGD-Las as revealed by MTT assay. This indicates that the most important interaction between RGD-Las and tumor cells

Journal of PeptideScience

is between αvβ3 and RGD. Although the <H> of RGD-Las was lower than that of temporin-La, the anticancer efficiency was higher, so we considered that the ligand-targeting effect and electrostatic interactions contributed to the increased anticancer activity.

In our study, the new chimeric peptides acted in three processes. Electrostatic interactions between the chimeric peptides and cancer cells were one of the processes and required +3 or +4 net positive charges. The RGD motif of the chimeric peptides targets the peptide to αvβ3 molecules on the cell membrane. The amphipathic structure allows pore formation, causing cell death. We observed the binding of RGD-Las to the cell membrane by the time-dependent morphological changes under a confocal microscope. We found that the process of peptide binding and penetrating the membrane was so fast that all the cells in the area were dead within 1 h. Cells were quickly filled with fluorescent dye (FITC), suggesting that these cationic peptides bind to intracellular molecules (such as DNA and RNA) that are strongly negative. In the time course, many cell fragments exfoliated, and these fragments were also strongly fluorescent (Figure 5). The peptides were bound firmly to the cell membranes, and nuclear condensation was present. Although we did not see strong fluorescence intensity concentrating at punctuate sites on the cell membrane, this may relate to the distribution of αvβ3 over the tumor cell membrane. We also compared morphologic changes of the cell membrane induced by temporin-La and RGD-Las using SEM. Pores were seen around the whole surface of the cells treated with temporin-La, whereas pores were seen only around the nucleus in cells treated with RGD-Las. Some microvilli were clearly visible at the nuclear regions of cells treated by RGD-Las. Membrane disruption was not equal around the cell surface after RGD-Las treatment. These results suggested that RGD-Las may have specific membrane disrupting activity for αvβ3-positive cancer cells. RGD-Las targeted SMMC7721 cells most strongly, and these cells express high levels of αvβ3 in the membrane. Although the cells were treated for 30 min with both temporin-La and RGD-Las, cells treated with RGD-Las were more damaged. As no apoptotic mechanism could be detected on tumor cells treated with RGD-Las, a membrane-disturbing action seems to be the major mechanism for cell death. At the same time, we observed a lot of pores on the damaged cell membranes, consistent with the carpet model mechanism.

In conclusion, RGD-Las shows high cytotoxicity against tumor cells *in vitro* without hemolysis.

Acknowledgements

The authors wish to thank Yuanhua Yu for providing the tumor cell lines and Xinrui Wang and Yang Li for their generous assistance in providing experimental devices.

References

1 Maino DM, Tran S, Mehta F. Side effects of chemotherapeutic oculotoxic agents: a review. *Clin. Eye Vis. Care.* 2000; **12**: 113–117.
2 Verrills NM, Kavallaris M. Drug resistance mechanisms in cancer cells: a proteomics perspective. *Curr. Opin. Mol. Ther.* 2003; **5**: 258–265.
3 Tan DS, Gerlinger M, Teh BT, Swanton C. Anti-cancer drug resistance: understanding the mechanisms through the use of integrative genomics and functional RNA interference. *Eur. J. Cancer* 2010; **46**: 2166–2177.
4 Calcagno AM, Ambudkar SV. Molecular mechanisms of drug resistance in single-step and multi-step drug-selected cancer cells. *Methods Mol. Biol.* 2010; **596**: 77–93.
5 Monsuez JJ, Charniot JC, Vignat N, Artigou JY. Cardiac side-effects of cancer chemotherapy. *Int. J. Cardiol.* 2010; **144**: 3–15.
6 Zasloff M. Antimicrobial peptides of multicellular organisms. *Nature* 2002; **415**: 389–395.
7 Hoskin DW, Ramamoorthy A. Studies on anticancer activities of antimicrobial peptides. *Biochim. Biophys. Acta* 2008; **1778**: 357–375.
8 Wang KR, Zhang BZ, Zhang W, Yan JX, Li J, Wang R. Antitumor effects, cell selectivity and structure–activity relationship of a novel antimicrobial peptide polybia-MPI. *Peptides* 2008; **29**: 963–968.
9 Wang C, Li HB, Li S, Tian LL, Shang DJ. Antitumor effects and cell selectivity of temporin-1CEa, an antimicrobial peptide from the skin secretions of the Chinese brown frog (*Rana chensinensis*). *Biochimie* 2012; **94**: 434–441.
10 Kim S, Kim SS, Bang YJ, Kim SJ, Lee BJ. *In vitro* activities of native and designed peptide antibiotics against drug sensitive and resistant tumor cell lines. *Peptides* 2003; **24**: 945–953.
11 Lienkamp K, Tew GN. Synthetic mimics of antimicrobial peptides—a versatile ring-opening metathesis polymerization based platform for the synthesis of selective antibacterial and cell-penetrating polymers. *Chemistry* 2009; **15**: 11784–11800.
12 Koczulla AR, Bals R. Antimicrobial peptides: current status and therapeutic potential. *Drugs* 2003; **63**: 389–406.
13 Rathinakumar R, Walkenhorst WF, Wimley WC. Broad-spectrum antimicrobial peptides by rational combinatorial design and high-throughput screening: the importance of interfacial activity. *J. Am. Chem. Soc.* 2009; **131**: 7609–7617.
14 He J, Anderson MH, Shi W, Eckert R. Design and activity of a 'dual-targeted' antimicrobial peptide. *Int. J. Antimicrob. Agents* 2009; **33**: 532–537.
15 Jiang Z, Vasil AI, Hale J, Hancock RE, Vasil ML, Hodges RS. Effects of net charge and the number of positively charged residues on the biological activity of amphipathic α-helical cationic antimicrobial peptides. *Adv. Exp. Med. Biol.* 2009; **611**: 561–562.
16 Hong SY, Park TG, Lee KH. The effect of charge increase on the specificity and activity of a short antimicrobial peptide. *Peptides* 2001; **22**: 1669–1674.
17 Yamamoto N, Tamura A. Designed low amphipathic peptides with α-helical propensity exhibiting antimicrobial activity via a lipid domain formation mechanism. *Peptides* 2010; **31**: 794–805.
18 Dathe M, Wieprecht T. Structural features of helical antimicrobial peptides: their potential to modulate activity on model membranes and biological cells. *Biochim. Biophys. Acta* 1999; **1462**: 71–87.
19 Iwasaki T, Ishibashi J, Tanaka H, Sato M, Asaoka A, Taylor D, Yamakawa M. Selective cancer cell cytotoxicity of enantiomeric 9-mer peptides derived from beetle defensins depends on negatively charged phosphatidylserine on the cell surface. *Peptides* 2009; **30**: 660–668.
20 Mader JS, Hoskin DW. Cationic antimicrobial peptides as novel cytotoxic agents for cancer treatment. *Expert Opin. Investig. Drugs* 2006; **15**: 933–946.
21 Dennison SR, Harris F, Bhatt T, Singh J, Phoenix DA. A theoretical analysis of secondary structural characteristics of anticancer peptides. *Mol. Cell. Biochem.* 2010; **333**: 129–135.
22 Dobrzynska I, Szachowicz-Petelska B, Sulkowski S, Figaszewski Z. Changes in electric charge and phospholipids composition in human colorectal cancer cells. *Mol. Cell. Biochem.* 2005; **276**: 113–119.
23 Yoon WH, Park HD, Lim K, Hwang BD. Effect of O-glycosylated mucin on invasion and metastasis of HM7 human colon cancer cells. *Biochem. Biophys. Res. Commun.* 1996; **222**: 694–699.
24 Marquez M, Nilsson S, Lennartsson L, Liu Z, Tammela T, Raitanen M, Holmberg AR. Charge-dependent targeting: results in six tumor cell lines. *Anticancer Res.* 2004; **24**: 1347–1351.
25 Han WY, Zhao RL, Han JY, Lei LC, Sun CJ, Feng X, Jiang LN, Qiao HW, Cai LJ. Molecular cloning of two novel temporins from *Lithobates catesbeianus* and studying of their antimicrobial mechanisms. *Prog. Biochem. Biophys.* 2009; **36**: 1064–1070.
26 Wang Z, Wang G. APD: the Antimicrobial Peptide Database. *Nucleic Acids Res.* 2004; **32**: D590–592.
27 Fauchère J, Pliska V. Hydrophobic parameters-pi of amino-acid side-chains from the partitioning of *N*-acetyl-amino-acid amides. *Eur. J. Med. Chem.* 1983; **8**: 369–375.
28 Eisenberg D, Weiss RM, Terwilliger TC. The helical hydrophobic moment: a measure of the amphiphilicity of a helix. *Nature* 1982; **299**: 371–374.
29 Kyte J, Doolittle RF. A simple method for displaying the hydropathic character of a protein. *J. Mol. Biol.* 1982; **157**: 105–132.

30 Wilkins MR, Gasteiger E, Bairoch A, Sanchez JC, Williams KL, Appel RD, Hochstrasser DF. Protein identification and analysis tools in the ExPASy server. *Methods Mol. Biol.* 1999; **112**: 531–552.
31 Tossi A, Sandri L, Giangaspero A. Amphipathic, α-helical antimicrobial peptides. *Biopolymers* 2000; **55**: 4–30.
32 Gautier R, Douguet D, Antonny B, Drin G. HELIQUEST: a web server to screen sequences with specific α-helical properties. *Bioinformatics* 2008; **24**: 2101–2102.
33 Tamura K, Dudley J, Nei M, Kumar S. MEGA4: Molecular Evolutionary Genetics Analysis (MEGA) software version 4.0. *Mol. Biol. Evol.* 2007; **24**: 1596–1599.
34 Deleage G, Combet C, Blanchet C, Geourjon C. ANTHEPROT: an integrated protein sequence analysis software with client/server capabilities. *Comput. Biol. Med.* 2001; **31**: 259–267.
35 Kerwin SM. CHEMBIOOFFICE Ultra 2010 suite. *J. Am. Chem. Soc.* 2010; **132**: 2466–2467.
36 Bignami GS. A rapid and sensitive hemolysis neutralization assay for palytoxin. *Toxicon* 1993; **31**: 817–820.
37 Mangoni ML, Rinaldi AC, Di Giulio A, Mignogna G, Bozzi A, Barra D, Simmaco M. Structure–function relationships of temporins, small antimicrobial peptides from amphibian skin. *Eur. J. Biochem.* 2000; **267**: 1447–1454.
38 Simmaco M, Mignogna G, Canofeni S, Miele R, Mangoni ML, Barra D. Temporins, antimicrobial peptides from the European red frog *Rana temporaria*. *Eur. J. Biochem.* 1996; **242**: 788–792.
39 Carter HB, Coffey DS. Cell surface charge in predicting metastatic potential of aspirated cells from the Dunning rat prostatic adenocarcinoma model. *J. Urol.* 1988; **140**: 173–175.
40 Papo N, Shai Y. Can we predict biological activity of antimicrobial peptides from their interactions with model phospholipid membranes? *Peptides* 2003; **24**: 1693–1703.
41 Liu S. Radiolabeled cyclic RGD peptides as integrin α(v)β(3)-targeted radiotracers: maximizing binding affinity via bivalency. *Bioconjug. Chem.* 2009; **20**: 2199–2213.
42 Dijkgraaf I, Beer AJ, Wester HJ. Application of RGD-containing peptides as imaging probes for αvβ3 expression. *Front. Biosci.* 2009; **14**: 887–899.
43 Frochot C, Di Stasio B, Vanderesse R, Belgy MJ, Dodeller M, Guillemin F, Viriot ML, Barberi-Heyob M. Interest of RGD-containing linear or cyclic peptide targeted tetraphenylchlorine as novel photosensitizers for selective photodynamic activity. *Bioorg. Chem.* 2007; **35**: 205–220.
44 Gibrat JF, Garnier J, Robson B. Further developments of protein secondary structure prediction using information theory. New parameters and consideration of residue pairs. *J. Mol. Biol.* 1987; **198**(3): 425–443.

